

Accurate skin dose measurements using radiochromic film in clinical applications

S. Devic,^{a)} J. Seuntjens, W. Abdel-Rahman, M. Evans, M. Olivares, and E. B. Podgorsak
Medical Physics Department, McGill University Health Centre, Montreal, Quebec, Canada

Té Vuong

Department of Radiation Oncology, McGill University Health Centre, Montreal, Quebec, Canada

Christopher G. Soares

Division of Ionizing Radiation, National Institute of Standards and Technology, Gaithersburg, Maryland 20899

(Received 12 August 2005; revised 1 December 2005; accepted for publication 1 February 2006; published 29 March 2006)

Megavoltage x-ray beams exhibit the well-known phenomena of dose buildup within the first few millimeters of the incident phantom surface, or the skin. Results of the surface dose measurements, however, depend vastly on the measurement technique employed. Our goal in this study was to determine a correction procedure in order to obtain an accurate skin dose estimate at the clinically relevant depth based on radiochromic film measurements. To illustrate this correction, we have used as a reference point a depth of $70\ \mu$. We used the new GAFCHROMIC[®] dosimetry films (HS, XR-T, and EBT) that have effective points of measurement at depths slightly larger than $70\ \mu$. In addition to films, we also used an Attix parallel-plate chamber and a home-built extrapolation chamber to cover tissue-equivalent depths in the range from $4\ \mu$ to 1 mm of water-equivalent depth. Our measurements suggest that within the first millimeter of the skin region, the PDD for a 6 MV photon beam and field size of $10 \times 10\ \text{cm}^2$ increases from 14% to 43%. For the three GAFCHROMIC[®] dosimetry film models, the 6 MV beam entrance skin dose measurement corrections due to their effective point of measurement are as follows: 15% for the EBT, 15% for the HS, and 16% for the XR-T model GAFCHROMIC[®] films. The correction factors for the exit skin dose due to the build-down region are negligible. There is a small field size dependence for the entrance skin dose correction factor when using the EBT GAFCHROMIC[®] film model. Finally, a procedure that uses EBT model GAFCHROMIC[®] film for an accurate measurement of the skin dose in a parallel-opposed pair 6 MV photon beam arrangement is described. © 2006 American Association of Physicists in Medicine. [DOI: 10.1118/1.2179169]

Key words: clinical dosimetry, skin dose, surface dose, radiochromic film

I. INTRODUCTION

The skin-sparing effect for high-energy γ - and x-ray photons may be reduced or even lost, if the beam is contaminated with electrons and/or low-energy photons. Since the skin dose in treatment of deep-seated tumors may be the limiting factor in the delivery of high tumor doses, the dose distribution in the buildup region should be known. The relevant dose specification depth depends on the biological effect considered. For skin erythema the basal cell layer is of interest, while at higher doses the damage is related to deeper layers of the skin.¹ According to the ICRP² and the ICRU,³ the skin depth recommended for practical dose assessments is at 0.07 mm, and this depth generally corresponds to the interface between the epidermis and dermis layers of the skin. In this work, we use the recommended depth of $70\ \mu\text{m}$ only as a reference point for illustrative purposes. Since it is well known that the thickness of the epidermis varies throughout the human body,⁴ e.g., from 0.05 for the eyelid to 1.5 mm for sole of the foot, the clinically relevant depth for skin dose determination should be defined by the radiation oncologist on a case by case basis.

The surface dose is defined as the dose deposited at the boundary between the air and the phantom. Since the dose is a scalar quantity, the surface dose can be defined as the energy deposited within an infinitesimally small mass of tissue at the surface of the phantom. However, there is no dosimeter that has an infinitesimally small sensitive volume, and the surface dose by definition is inherently difficult to measure. The effective point of measurement of most commonly used dosimeters ranges from several micrometers of water-equivalent thickness (Capintec PS-033, MD-810 GAFCHROMIC[®] film) to a few millimeters (Roos, Exradin 11).⁵ For practical reasons, one may define the surface dose as the dose measured by one of the dosimeters used for surface dose measurements. Although such dosimeters may have a very shallow effective point of measurement, the derived surface dose only reflects the dose measured at the effective point of measurement for any particular dosimeter.

Since the conditions of charged particle equilibrium do not exist in the buildup region, the choice of the measurement device is of great importance. A variety of dosimeters can be used, such as fixed-separation parallel-plate

chambers,^{6–12} TLDs,^{13–17} diodes,^{18,19} and MOSFET²⁰ devices. However, a substantial degree of variance can occur across a field, particularly in the case of large fields with various angles incident on the body surface. The reference against which surface dose measurements are usually compared is the extrapolation chamber.^{21–23} However, measurements with the extrapolation chamber are time consuming, as each dose value is obtained by extrapolating several measurements to the zero volume. On the other hand, Gerbi has shown²⁴ that the commercially available fixed-separation parallel-plate Attix chamber can provide surface dose measurements with an accuracy ranging from +0.5% for a 6 MV photon beam to –0.5% for a 24 MV photon beam. While these two ionization chambers work well in the experimental environment, they are impractical for clinical applications when the surface or skin dose needs to be measured on a particular patient.

The introduction of radiochromic films has alleviated some of the problems experienced with conventional radiation dosimeters. The high spatial resolution and low spectral sensitivity of radiochromic films make them ideal for the measurement of dose distributions in regions of a high dose gradient in radiation fields.^{25–28} Although the sensitivity of the MD-55 model GAFCHROMIC[®] dosimetry film is relatively high, its dose response range is often too low for applications in everyday clinical practice. Nevertheless, this radiochromic film model has been extensively used for surface and skin dose measurements in various clinical situations.^{29–32} Three recent new radiochromic film models, the XR-T, HS, and EBT have been introduced by International Specialty Products (Wayne, NJ). In this paper, certain commercially available products are referred to by name. These references are for informational purposes only and do not imply that these are the best or only products available for the purpose, and do not imply endorsement by the National Institute of Standards and Technology. The EBT model has two sensitive layers, whereas the HS model has a single sensitive layer. Both film models were designed for two-dimensional dose measurements in high-energy photon beams (above 1 MeV). On the other hand, the XR-T model has a single sensitive layer containing high atomic number materials, intended to compensate for the lower absorption cross section of its organic active layer when irradiated with low-energy photons (below 0.1 MeV).

The goal of our study was to investigate the dose deposition within the first millimeter of the build-up region lacking the charged particle equilibrium conditions, and the last millimeter of the build-down region lacking a backscatter contribution to the dose deposition, within a Solid Water phantom exposed to a 6 MV photon beam. In the build-up region, we measured the percent depth dose (PDD) in an SSD setup with a $10 \times 10 \text{ cm}^2$ field at the surface using the Attix parallel-plate ionization chamber, a homemade extrapolation chamber, various GAFCHROMIC[®] film models (HD-810, EBT, HS, and XR-T), and TLDs. The range of the effective points of measurement for dosimeters used in this study was from 0.004 mm (for the HD-810 GAFCHROMIC[®] film model) up to 1.2 mm (for the Attix chamber covered with

four unexposed and developed layers of XV-2 radiographic films). We compared our measurements to Monte Carlo simulations of dose deposition within a water phantom for the same beam quality. In the build-down region, the PDD was measured using EBT model radiochromic filmstrips, positioned within the solid water phantom along the beam axis.

Most of the existing forward-based treatment planning systems (TPS³) calculate dose distributions using the beam data measured at the depth of dose maximum and beyond, and may estimate the dose in the buildup region by extrapolating measured data toward the surface by using fitted functions as an approximation. Consequently, most of the commercially available TPS calculate the exit doses under the full scatter conditions and cannot accurately provide the entrance skin doses. This creates an even more complex problem when entrance and exit aspects of beams, such as these found in parallel opposed set-ups, are encountered. Following the same approach that Nilsson¹⁴ developed for TLDs, we determined correction factors to obtain a skin dose at a depth of $70 \mu\text{m}$, while using the new high sensitive GAFCHROMIC[®] film (models HS, EBT, and XR-T), the latter having an effective point of measurement at a slightly deeper depth. We have also demonstrated that skin dose corrections for the effective point of measurement in the build-down region are negligible for the radiochromic film models used.

We also present clinically relevant correction factors for the EBT model GAFCHROMIC[®] film related to the skin dose correction factors as a function of the field size (from $5 \times 5 \text{ cm}^2$ to $30 \times 30 \text{ cm}^2$) for a 6 MV photon beams. A practical procedure, which uses the EBT model GAFCHROMIC[®] film for an accurate measurement of the skin dose in a parallel-opposed pair 6 MV photon beam arrangement is presented.

II. METHODS AND MATERIALS

A. Phantom and irradiation procedures

All dosimeters were placed on the surface of a phantom consisting of certified Solid Water phantom slabs (RMI, Model-457) having a physical density of 1.04 g/cm^3 in a source-surface distance (SSD) of 100 cm. Reference measurements were carried out by placing the dosimeters at a depth of 1.5 cm (depth of maximum dose deposition, z_{max}) in solid water, in a SSD setup. Measurements were carried out by irradiating the dosimeters at the phantom surface and at z_{max} in the phantom with a 6 MV photon beam using a Varian 2300 C/D accelerator (Varian, Palo Alto, CA).

B. Radiochromic films

The XR-T, HS, and EBT GAFCHROMIC[®] film models were developed as a more sensitive and more uniform alternative to the standard MD-55 model GAFCHROMIC[®] film. The HS and XR-T films employ similar active components as the GAFCHROMIC[®] HD-810 and GAFCHROMIC[®] MD-55 films. A diagram of the radiochromic film structures used in our study is given in Fig. 1. For both HS and XR-T

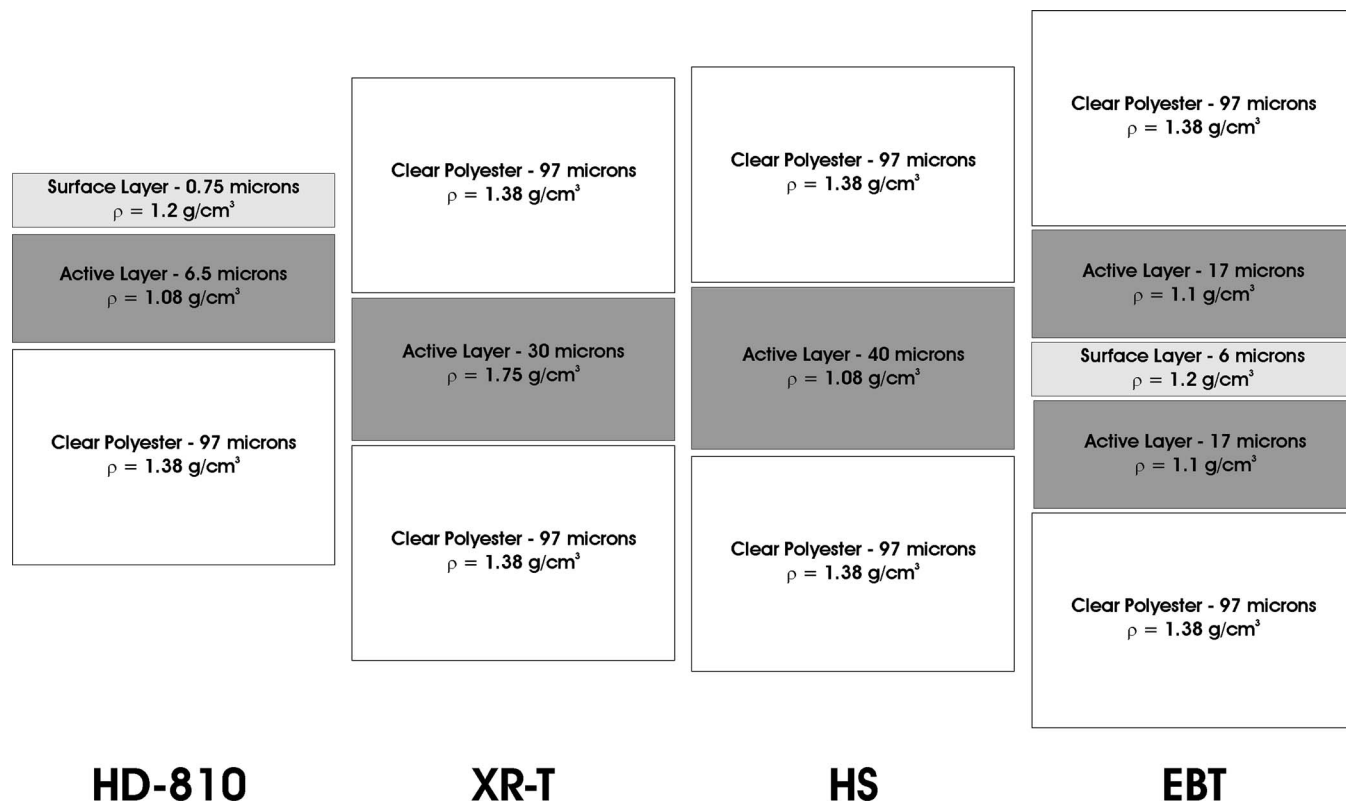


FIG. 1. Structures of GAFCHROMIC[®] film models used in this study.

models, GAFCHROMIC[®] films the active layer is sandwiched between two sheets of clear, transparent polyester, having a thickness of 97 μm and a density of 1.38 g/cm^3 . The thicknesses of the active layer in the GAFCHROMIC[®] HS film model is about 40 μ and in the XR-T film about 30 μ , with physical densities of 1.08 g/cm^3 for the HS and 1.75 g/cm^3 for the XR-T films. The structure of the new EBT film model is more complex than that of the HS model, and consists of two sensitive layers, each having a thickness of 17 μm and separated by a 6 μm thick surface layer, all sandwiched between two 97 μm clear polyester sheets. To extend the range of measurements to shallower depths, we also used the HD-810 model GAFCHROMIC[®] film. Its sensitivity is very low for clinical applications, but its effective point of measurement is at a depth of 4.4 microns and represents the shallowest point we were able to establish with our dosimeters. The effective points of measurement in the case of radiochromic films were assumed to be at the center of the sensitive layer of the film, and scaled by density they are 0.0153 g/cm^2 for the HS film, 0.0153 g/cm^2 for the EBT film, and 0.0157 g/cm^2 for XR-T GAFCHROMIC[®] films. We also assumed that the dose deposition within the sensitive layer is increasing monotonously with increasing thickness of the sensitive layer.

The change in optical density following dose deposition in GAFCHROMIC[®] films may be measured with transmission densitometers, film scanners, or spectrophotometers.³³ For GAFCHROMIC[®] film HD-810, HS, and XR-T models, the Nuclear Associates Radiochromic Densitometer Model

37-443 was used. This densitometer is especially suitable for spot measurements and it employs an optimum red LED light source and a matched filter to measure in a narrow band centered at about 670 nm. This corresponds very closely to the wavelength of the major peak in the spectrum of the photopolymer. The absorption spectrum of the new EBT film model exhibits a similar shape to its predecessors with the absorption peaks shifted toward shorter wavelengths, and with the maximum absorption band centered at about 633 nm.³⁴ For measurements with the EBT (Prototype A) GAFCHROMIC[®] film model, we used an Agfa Arcus II flatbed document scanner.³⁴

1. Buildup region measurements

The buildup region measurements were carried out with four different experiments: one for each radiochromic film model used. For every film model, we placed 5 pieces of film next to each other on the plane surface of the phantom and five film pieces next to each other on the plane at 1.5 cm depth for the reference dose measurement at the same time. Film pieces were arranged around the center of the field at both planes. The film pieces had a size of $2 \times 2.5 \text{ cm}^2$. To achieve a better than 5% dose uncertainty on the phantom surface (the expected percent dose value was estimated to be 15%) we delivered 600 Gy to HD-810, 50 Gy to XR-T, 30 Gy to HS, and 10 Gy to EBT (prototype A). The net

optical densities (NetOD) of the irradiated films were converted to absorbed dose using calibration curves determined previously.³⁴

2. Build-down region measurements

EBT film strips (3 cm wide and 23 cm long) were positioned between two pieces of solid water phantom material. The overall phantom size was $20 \times 20 \times 20$ cm³ and we created a 3 cm wide by 0.215 mm deep indent throughout the bottom half of the phantom to avoid air gaps between the solid water phantom surface and the radiochromic film. To avoid the influence of the precision with which one is able to accurately cut a film piece on a built-down region measurement, a 3 cm piece of film protruded from the phantom into the air in the direction away from the source. The downstream surface of the phantom was marked at the edge of the film surface for future reference. We delivered 6 Gy to the depth of maximum dose in a SSD setup with the field size at the phantom surface of 10×10 cm² and a gantry angle of 90° to simplify the measurement setup. Three film strips were exposed and for every film strip a *NetOD*³³ as a function of depth was determined. Film strips were scanned with a 0.1 mm/pixel scanning resolution. The region of interest over which the NetOD was calculated for each film strip was 1 mm by 1 mm (10 pixels \times 10 pixels). Averaged depth NetOD curves were converted to dose and normalized to the dose maximum to obtain the PDD data.

3. Field size dependence of the skin dose correction factors

In order to estimate the influence of the field size on the PDD curves in the buildup and build-down regions of the Solid Water phantom, we repeated the experiments with EBT GAFCHROMIC® film model for the following square field sizes: 5, 10, 15, 20, 25, and 30 cm. For buildup region measurements, single 5×5 cm² EBT pieces of film were placed at the surface of the solid water phantom and at the depth of maximum dose deposition. The region of interest used for the NetOD calculation was 5×5 mm² in the center of the 5×5 cm² film pieces. For the build-down measurements, a single EBT model film strip was irradiated to a dose of 6 Gy delivered at z_{\max} using the same setup as described previously for each field size.

C. Extrapolation chamber

The surface PDD was measured in solid water with the phantom-embedded extrapolation chamber (PEEC) originally designed for reference dosimetry measurements in our center.³⁵ The PEEC has parallel-plate geometry and the electrode separation can be varied continuously from a fraction of a mm to about 10 mm. To allow for measurements at the phantom surface we used a removable entrance window made of a thin aluminized Mylar (polyethylene terephthalate) foil stretched between two Delrin (polyoxymethylene) rings.³⁶ The combined thickness of the Mylar layer and the thin conducting aluminum layer is 50 μ m. When scaled by

the physical densities of its components, the effective point of measurement for the extrapolation chamber, assumed to be at the bottom of the entrance window electrode, was calculated to be 0.0069 g/cm².

D. Attix parallel-plate ionization chamber

Measurements with the Attix parallel-plate ionization chamber (RMI Model 449, Middleton, WI) were performed at two depths in phantom: the surface and at depth of z_{\max} at bias voltages of +300 V and -300 V. To further reconstruct the PDD curve within the buildup region extending up to one millimeter, we added one, two, three, and four layers of unexposed and developed XV-2 Kodak Ready pack films, each having a thickness of 0.0257 g/cm². In this way, we measured PDD values for 10×10 cm² field size at effective depths of 48 μ (the Attix chamber alone) and 0.0305, 0.0562, 0.0819, and 0.1176 cm (or g/cm²) for one, two, and three sheets of the XV-2 film, respectively. As in the case of the extrapolation chamber, the effective point of measurement was assumed to be at the bottom of the entrance window electrode.

The charge was measured with a Keithley 6517A Electrometer (Cleveland, OH). Every signal represents an average of five readings at a given voltage corrected for the output variation by the normalized reading of a monitor chamber positioned at a depth of 15 cm within the same solid water phantom. The small polarity effect within the buildup region for the Attix parallel-plate ionization chamber has been confirmed,²⁴ being the highest (3.8%) at the surface.

E. TLD measurements

The TLD dosimetry system consisted of a TLD reader (model 3500; Harshaw Chemical Company, Solon, OH) and dosimeters in the form of TLD chips. Lithium fluoride (LiF) crystals doped with magnesium and titanium (Harshaw Chemical Co, Solon, OH) having two different nominal thicknesses (0.15 and 0.4 mm) with a nominal surface area of 3.15×3.15 mm² were used.

Three TLDs have been positioned at the surface and another three TLDs of the same thickness have been positioned at the same time at depth of the dose maximum. All TLDs were calibrated by exposure to a known dose at the depth of dose maximum in solid water before and after each surface dose measurement. Based on this, an interpolated individual calibration factor was assigned to each TLD. Subsequently, using this calibration method, the surface doses obtained for the two different thicknesses of TLDs were determined. The TLDs were handled with vacuum tweezers using a plastic nozzle to avoid scratching the surface of the chips. All experiments were performed with doses of 1 Gy to avoid known problems with the supralinearity of LiF.

The effective point of measurement has been determined as one-half of the measured TLD thickness scaled by density. Since the TLD chips are very fragile, we have measured the mass of the TLD chips (in g) and then determined the TLD chip surface area (in cm²) by taking a digital image of the

TABLE I. Effective points of measurement as well as ratios of stopping power ratios at the effective point of measurement (z_{eff}) and at z_{max} for dosimeters used in this study.

Dosimeter	Depth scaled by density (g/cm ²)	Equivalent depth in water (μm)	$\left(\frac{L_{\Delta}}{\rho}\right)_{\text{det}}^{\text{wat}}(z_{\text{eff}})/\left(\frac{L_{\Delta}}{\rho}\right)_{\text{det}}^{\text{wat}}(z_{\text{max}})$
HD-810 GAFCHROMIC [®] film	0.0004	4	0.9996
Attix chamber	0.0048	48	1.012 ^a
Extrapolation chamber	0.0069	69	1.010 ^a
HS GAFCHROMIC [®] film	0.0153	153	0.9993
EBT GAFCHROMIC [®] film	0.0153	153	0.9997
XR-T GAFCHROMIC [®] film	0.0157	157	0.9997
TLD-100 (0.15 mm)	0.0185	185	1.002
Attix chamber + 1 XV-2 sheet	0.0305	305	1.009 ^a
TLD-100 (0.4 mm)	0.0496	496	1.001
Attix chamber + 2 XV-2 sheets	0.0562	562	1.007 ^a
Attix chamber + 3 XV-2 sheets	0.0819	819	1.006 ^a
Attix chamber + 4 XV-2 sheets	0.1176	1176	1.005 ^a

^aData from Ref. 36.

chip surface. Effective points of measurement for the two TLD chip types have been determined as 0.0185 g/cm² for the 0.15 mm nominal thickness and 0.0496 g/cm² for the 0.4 mm nominal thickness.

The change in the ratio of stopping power ratios water to LiF for the 6 MV beam used in this study was calculated by the Monte Carlo simulations and was found to be less than 0.3% and was neglected in the surface PDD calculations for the TLD detectors. The reproducibility expressed as the sample standard deviation on a dose measurement at a given depth based on the six TLDs each with their individual calibration factor amounted to 2%.

F. Monte Carlo calculations

The DOSRZnrc/EGSnrc Monte Carlo (MC) code^{37,38} was used to calculate the absorbed dose in the buildup region of the 6 MV photon beam irradiating the water phantom. The Varian 2300 (C/D) linac was modeled using the BEAMnrc/EGSnrc MC code based on specifications obtained from the manufacturer. The electron energy at the linac exit window was optimized by a comparison of percentage depth dose at depths equal to and larger than the depth of the maximum dose as measured in water with an IC-10 ionization chamber. Using this primary energy (6 MeV for the 6 MV beam), particle phase spaces at SSD 100 cm were collected for 10 × 10 cm² field and used as sources for the transport calculations in the water phantom. In most calculations we used a photon transport cutoff of 0.521 MeV and an electron kinetic energy transport cutoff of 0.010 MeV. To ensure accurate electron transport, DOSRZnrc was run using exact boundary crossing algorithm, the PRESTA-II electron transport algorithm and with relativistic spin effects in the modeling of multiple scattering. The scoring regions chosen for the accurate calculation of build-up dose were 0.001 g/cm² thick with their centers at depths of 0.00075, 0.002, 0.00479, 0.01013, 0.0267, 0.0587, and 0.100 g/cm² for the 6 MV x-ray beam.

The SPRRZnrc/EGSnrc user code^{37,38} was used to calculate ratios of stopping power ratios water to detector material, $(L_{\Delta}/\rho)_{\text{det}}^{\text{wat}}$, at various depths in the dose buildup region corresponding to physical depths of the effective points of measurement and at z_{max} for all dosimeters used in this study. These ratios have been used to convert the measured detector response ratios to the surface PDD values for every particular dosimeter.

III. RESULTS AND DISCUSSION

A. Effective point of measurement

To estimate the clinically relevant skin dose, we performed dose measurements within the first millimeter of the buildup region for 6 MV photon beam using an array of radiation detectors, including an Attix parallel-plate ionization chamber, extrapolation chamber, HD-810, EBT, HS and XR-T GAFCHROMIC[®] films, and TLDs. Table I summarizes the effective point of measurement for dosimeters used in our study. For parallel-plate ionization chambers, the effective point of measurement is at a depth, that corresponds to the entrance electrode window thickness scaled by physical density of the electrode material. On the other hand, for radiochromic films and TLDs, the effective point of measurement was defined at the middle of the sensitive layer for a particular dosimeter, scaling by appropriate density all layers above the effective point. The last column in Table I represents ratio of stopping power ratios at the effective point of measurement and the depth of dose maximum for different dosimeters used in this study.

It was shown by Abdel-Rahman *et al.*³⁶ that for a 6 MV photon beam the ratio of stopping power ratios water-air in the buildup region increases with decreasing depth from 1.000 at z_{max} to 1.012 at a depth of 50 μm . The PDDs for the Attix parallel-plate and extrapolation ionization chambers measured in this work represent the ratio of the two measured charge values multiplied by the ratio of the stopping power ratios water-air at two depths (the effective point of

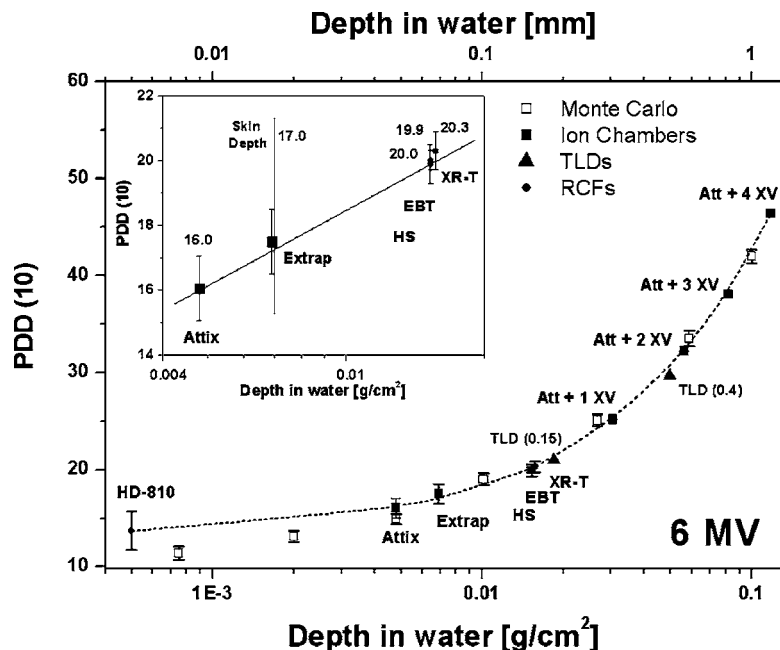


FIG. 2. Percent depth dose for a 6 MV photon beam within the first millimeter of the water phantom: solid symbols represent depth dose values measured with dosimeters indicated; open symbols correspond to Monte Carlo simulation data; the dashed line is guide for the eye. Inset: enlarged portion of the PDD curve used to derive entrance skin dose correction factors for GAFCHROMIC® film models used in this study.

measurement depth and the depth of dose maximum) obtained from Monte Carlo simulations.³⁶ Other chamber-dependent perturbation correction factors were ignored.

B. Buildup region percent depth dose

Results of our PDD measurements in the buildup region are presented in Fig. 2 for our array of dosimeters. The solid symbols correspond to PDD measurements normalized at a depth of z_{max} in the water phantom. The measurements are reported at depths scaled by density, given in Table I. The dashed line serves as a guide for the eye. Percentage uncertainties in measurements in terms of one standard deviation around the mean are shown on the graphs. The open symbols represent the results of Monte Carlo simulations. Figure 2 reveals that within the first millimeter of the buildup region, the PDD increases from 14% at a depth of 4 μ m to 43% at a depth of 1 mm, a 3-fold increase in terms of absolute dose.

The inset in Fig. 2 represents the first 0.2 mm of the phantom depth. The values indicated in the inset represent the PDD values for the given depths as read out with a given dosimeter. The skin depth was assumed to be at the reference point of 70 μ m, and the necessary corrections for the reliable estimate of the skin dose based upon the measurements with various GAFCHROMIC® dosimetry film models, as well as the other surface dose dosimeters, are summarized in Table II.

The correction factors for the skin dose estimation, given in Table II, suggest that there is a relatively large correction (15%–16%) that one should apply when using GAFCHROMIC® dosimetry films with 6 MV photon beams. Only the Attix parallel-plate ionization chamber will underestimate the skin dose and this by 6%. Depending on the TLD model used, corrections can be either 0.810 (a 19% change) for 0.15 mm thick or even 0.586 (a 41% correction) for 0.4 mm thick TLD chips. Corrections for the HD-810 GAFCHROMIC® film and the extrapolation chamber are not included in Table II because these dosimeters are impractical for clinical applications. Extrapolation chamber measurements are impractical because of the tedious procedure, even for experimental-type setups, while the HD-810 GAFCHROMIC® film model requires exposures that are well above clinically relevant doses.

Monte Carlo simulated PDD values agree well with measurement, except at very shallow depths, below approximately 10 μ . However, this discrepancy is well within the measurement uncertainty (14% relative experimental uncertainty) when the HD-810 GAFCHROMIC® film model is used and the Monte Carlo uncertainty due to the relatively large electron kinetic energy transport cutoff used (0.010 MeV) for such a small scoring region.

TABLE II. Correction factors necessary to scale the dose measured at the effective point of measurement for a given detector used in this study to the clinically relevant skin dose depth of 70 μ m.

	Skin (70 μ m)	Attix	EBT	HS	XR-T	TLD (0.15)	TLD (0.4)
PDD (z_{eff} , 10, 100, 6 MV)	17.0	16.0	19.9	20.0	20.3	21	29
Correction	1.000	1.062	0.854	0.850	0.837	0.810	0.586

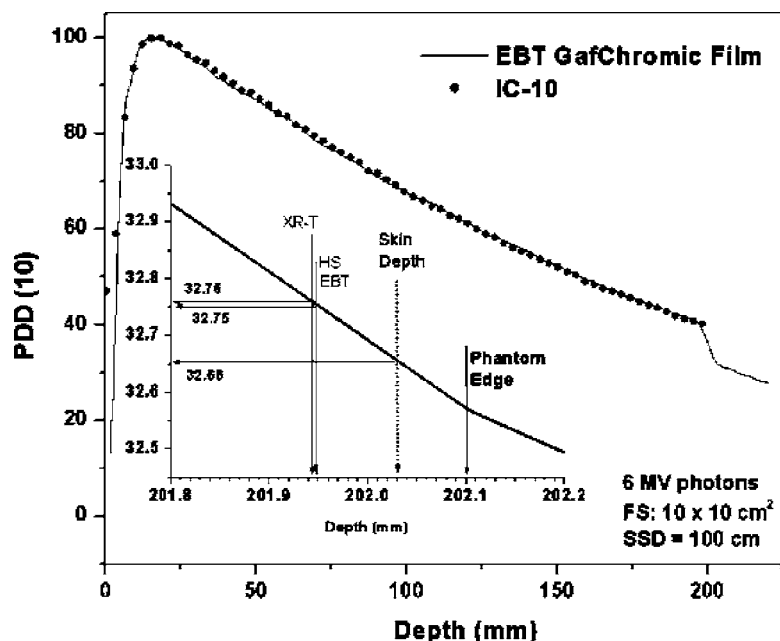


FIG. 3. Percent depth dose curve in the build-down region for a 6 MV photon beam; the inset represents the enlarged last 0.3 mm of the phantom.

C. Build-down region percent depth dose

Results of PDD measurements in the build-down region are presented in Fig. 3. The symbols represent PDD measurements normalized at the depth of z_{max} in the water phantom with an IC-10 ionization chamber. The solid line represents the PDD curve reconstructed from the EBT strip measurement. The measured build-down effect of 6.5% over 10 mm is in good agreement with previously published data.³⁹ Figure 3 represents a confirmation of the film strip method for convenient PDD reconstruction, even within the buildup and the build-down region.

The inset of Fig. 3 represents the last 0.3 mm of the phantom depth. The values indicated in the inset represent the PDD values for given depths as read out from the PDD line measured with the EBT film strip. The depth of the skin was again assumed to be at 70 μ m, and the necessary corrections for the reliable estimate of the exit skin dose based upon the measurements with various GAFCHROMIC® film models, are given in Table III.

Based on the results of Fig. 3 and Table III, we conclude that if any of the three GAFCHROMIC® film models are used for the estimation of the exit skin dose, a maximum correction of 0.3% would be required if the skin depth was assumed to be at 70 μ m; a correction that is well within the experimental uncertainty of the measured PDD values and one that can be ignored.

TABLE III. Exit skin dose correction factors for GAFCHROMIC® film models used in this study.

GAFCHROMIC® film model	Skin (70 μ m)	EBT	HS	XR-T
PDD ($z, 10, 100, 6$ MV)	32.66	32.75	32.75	32.76
Correction	1.000	0.997	0.997	0.997

D. Field size effect on buildup and build-down percent depth doses

To investigate the field size influence on the correction factors for accurate skin dose measurements, we have performed measurements with the EBT model GAFCHROMIC® film. The results of this analysis are summarized in Table IV. It is apparent that the correction factors do not change with field size and remain negligible for the exit skin dose estimates. On the other hand, a relatively small increase in correction factor has been observed for the entrance skin dose corrections for field sizes above 10 \times 10 cm². However, for field sizes above 10 \times 10 cm², the change in the correction factors is of the order of 4%, whereas for a field size of 5 \times 5 cm², the change amounts to 15%.

E. Clinically relevant case

As an example, we consider a clinically relevant case where we intend to treat a patient having a separation of 20 cm using SSD setup, with an opposed pair of beams having a field size of 10 \times 10 cm². An assumption is made that both beams deliver 100 cGy at the depth of dose maximum, giving a mid-plane dose of 135.4 cGy, and that we are interested in the skin dose at the anterior surface of the patient. In this idealized case, the skin dose can be measured using the GAFCHROMIC® EBT film in two ways. The first method would be to position one piece of film at the anterior surface and deliver both beams. The other method might be to position the first film piece at the anterior surface of the patient and deliver the anterior beam only; then, place a second piece of film at the same location and deliver the posterior beam.

Based on the results presented in Table IV, we conclude that the dose delivered to the skin, at a reference depth of 70 μ m will be 17.0 cGy + 32.66 cGy = 49.66 cGy. In the first

TABLE IV. Field size dependence of the entrance and exit skin dose correction factors for the EBT model GAFCHROMIC[®] film. Note that exit PDDs and corresponding correction factors correspond to the 20 cm phantom thickness only.

Field Size (cm ²)	5 × 5	10 × 10	15 × 15	20 × 20	25 × 25	30 × 30
Entrance PDD (70 μm)	11.5	17.0	23.6	28.4	33.5	37.2
Entrance PDD (153 μm)	14.3	19.9	26.0	31.2	36.2	40.1
Entrance skin dose correction	0.804	0.854	0.908	0.910	0.925	0.928
Exit PDD (70 μm)	30.61	32.66	34.46	35.56	36.37	37.26
Exit PDD (153 μm)	30.67	32.75	34.36	35.63	36.48	37.33
Exit skin dose correction	0.998	0.997	0.997	0.998	0.997	0.998

case one would measure $19.9 \text{ cGy} + 32.75 \text{ cGy} = 52.65 \text{ cGy}$. In this type of measurement, one would overestimate the absolute dose value by 5%. However, by applying the correction factor for a given field size of 11% on the entrance skin dose, and assuming a constant 0.997 exit skin correction factor, one can obtain a more accurate skin dose estimate. By applying the same rationale for the GAFCHROMIC[®] HS and XR-T film models, and by using Tables II and III, one may expect that the uncorrected film measurements would give $20.0 \text{ cGy} + 32.75 \text{ cGy} = 52.75 \text{ cGy}$ for the HS film, and $20.3 \text{ cGy} + 32.76 \text{ cGy} = 53.06 \text{ cGy}$ for the XR-T GAFCHROMIC[®] film, or an overestimate in the skin dose of 6% and 7%, respectively.

IV. CONCLUSIONS

Our measurements suggest that within the first millimeter of the buildup region, the PDD for a 6 MV photon beam and field size of $10 \times 10 \text{ cm}^2$ increases from 14% to 40%. Accordingly, different dosimeters used for the surface dose estimates should be properly calibrated and necessary corrections applied in order to estimate accurately the skin dose for clinical applications. For the three different GAFCHROMIC[®] dosimetry film models, these corrections are 15% for EBT, 15% for HS, and 16% for XR-T model GAFCHROMIC[®] films if the clinically relevant skin depth was assumed to be at 70μ . Our measurements are in good agreement with Monte Carlo simulations, except at very shallow depths. The discrepancy that appears at depths of the order of $10 \mu\text{m}$ or less may be due to the relatively small thickness of the simulated scoring layers with respect to the range of the cutoff electron energies used in this work.

Our measurements have also shown that the skin dose correction for the effective point of measurement in the build-down region is of the order of 0.3% for all three GAFCHROMIC[®] film models over a range of field sizes from $5 \times 5 \text{ cm}^2$ to $30 \times 30 \text{ cm}^2$. However, in the build-up region, a change of the field size will result in a change of the entrance skin dose scaling factor for EBT GAFCHROMIC[®] film model from 0.80 for a $5 \times 5 \text{ cm}^2$ to 0.93 for a $30 \times 30 \text{ cm}^2$ field size.

We have also shown that by ignoring the skin dose correction factors, the skin dose estimate based on a single film piece measurement would overestimate the skin dose by 5% for the EBT, 6% for the HS, and 7% for the XR-T

GAFCHROMIC[®] film model. In conclusion, we would like to emphasize that one should know not only the effective measurement point of the device used for the skin dose measurement-but the overall PDD curve behavior within the first millimeter of the skin region as well. Then, following the skin depth specification of radiation oncologist one should be able to provide an estimate of the skin dose at the clinically relevant depth for a particular clinical case.

ACKNOWLEDGMENTS

We would like to thank Dr. David Lewis from ISP for useful discussions. J. S. is a research scientist of the National Cancer Institute Canada appointed with funds provided by the Canadian Cancer Society.

- ^{a)}Corresponding author: Slobodan Devic Ph.D., Department of Medical Physics, McGill University, Montreal General Hospital, 1650 avenue Cedar, L5-112, Montreal, Quebec H3G 1A4, Canada. Telephone: 514-934-8052; fax: 514-934-8229; electronic mail: devic@medphys.mcgill.ca
- ¹ICRP Publication 28, *The Principles and General Procedures For Handling Emergency and Accidental Exposures of Workers* (Pergamon, Oxford, 1978).
- ²ICRP Publication 60, *Recommendations of the International Commission on Radiological Protection*, Pergamon, Oxford, 1991.
- ³ICRU, "Determination of dose equivalents resulting from external radiation sources." Report No. 39, International Commission on Radiation Units and Measurement, Washington, DC, 1985.
- ⁴ICRP Publication 23, *Anatomical, Physiological and Metabolic Characteristics* (Pergamon, Oxford, 1975).
- ⁵"The use of plane parallel ionization chambers in high energy electron and photon beams," IAEA Technical Report 381, IAEA, Vienna, 1997.
- ⁶N. B. J. Tannous, W. F. Gagnon, and P. R. Almond, "Buildup region and skin-dose measurements for the Therac 6 Linear Accelerator for radiation therapy," *Med. Phys.* **8**, 378-381 (1981).
- ⁷J. A. Purdy, "Buildup/surface dose and exit dose measurements for a 6-MV linear accelerator," *Med. Phys.* **13**, 259-262 (1986).
- ⁸B. J. Gerbi and F. M. Khan, "Measurement of dose in the buildup region using fixed-separation plane-parallel ionization chambers," *Med. Phys.* **17**, 17-26 (1990).
- ⁹C. Fiorino, G. M. Cattaneo, A. del Vecchio, V. Fossati, and F. Volterrani, "Skin dose measurements for head and neck radiotherapy," *Med. Phys.* **19**, 1263-1266 (1992).
- ¹⁰H. Kubo, "Evaluations of two solid water parallel-plate chambers in high-energy photon and electron beams," *Med. Phys.* **20**, 341-345 (1993).
- ¹¹S. E. Burch, S. A. Parker, A. M. Vann, and J. C. Arazie, "Measurement of 6-MV X-ray surface dose when topical agents are applied prior to external beam radiation," *Int. J. Radiat. Oncol., Biol., Phys.* **38**, 447-451 (1997).
- ¹²S. Kim, C. R. Liu, T. C. Zhu, and J. R. Palta, "Photon beam skin dose analyses for different clinical setups," *Med. Phys.* **25**, 860-865 (1998).
- ¹³M. W. Charles and Z. U. Khan, "Implementation of the ICRP recommen-

- dation on skin dose measurement using thermoluminescent dosimeters," *Phys. Med. Biol.* **23**, 972–975 (1978).
- ¹⁴B. Nilsson and B. Sorcini, "Surface dose measurements in clinical photon beams," *Acta Oncol.* **28**, (1989) 537–542.
- ¹⁵T. Kron, A. Elliot, T. Wong, G. Showell, B. Clubb, and P. Metcalfe, "X-ray surface dose measurements using TLD extrapolation," *Med. Phys.* **20**, 703–711 (1993).
- ¹⁶P. M. Ostwald, T. Kron, C. S. Hamilton, and J. W. Denham, "Clinical use of carbon-loaded thermoluminescent dosimeters for skin dose determination," *Int. J. Radiat. Oncol., Biol., Phys.* **33**, 943–950 (1995).
- ¹⁷J. P. Lin, T. C. Chu, S. Y. Lin, and M. T. Liu, "Skin dose measurement by using ultra-thin TLDs," *Appl. Radiat. Isot.* **55**, 383–391 (2001).
- ¹⁸B. E. Bjärngard, P. Vadash, and T. Zhu, "Doses near the surface in high-energy x-ray beams," *Med. Phys.* **22**, 465–468 (1995).
- ¹⁹N. Jornet, M. Ribas, and T. Eudaldo, "In vivo dosimetry: Intercomparison between *p*-type based and *n*-type based diodes for the 16–25 MV energy range," *Med. Phys.* **27**, 1287–1293 (2000).
- ²⁰M. J. Butson, A. Rozenfeld, J. N. Mathur, M. Carolan, T. P. Y. Wong, and P. E. Metcalfe, "A new radiotherapy surface dose detector: The MOS-FET," *Med. Phys.* **23**, 655–658 (1996).
- ²¹D. E. Velkley, D. J. Manson, J. A. Purdy, and G. D. Oliver, "Build-up region of megavoltage photon radiation sources," *Med. Phys.* **2**, 14–19 (1975).
- ²²B. Nilsson and A. Montelius, "Fluence perturbation in photon beams under nonequilibrium conditions," *Med. Phys.* **13**, 191–195 (1986).
- ²³S. Cora and P. Francescon, "Accurate build-up and surface dose measurements of megavolt photon beams from variety of accelerators," *Phys. Medica* **11**, 17–22 (1995).
- ²⁴B. J. Gerbi, "The response characteristics of a newly designed plane-parallel ionization chamber in high-energy photon and electron beams," *Med. Phys.* **20**, 1411–1415 (1993).
- ²⁵W. L. McLaughlin, A. Miller, S. Fidan, K. Pejtersen, and W. B. Pedersen, "Radiochromic plastic film for accurate measurement of radiation absorbed dose and dose distributions," *Radiat. Phys. Chem.* **10**, 119–127 (1977).
- ²⁶W. L. McLaughlin, J. C. Humphreys, B. B. Radak, A. Miller, and T. A. Olejnik, "The response of plastic dosimeters to gamma rays and electrons at high absorbed dose rates," *Radiat. Phys. Chem.* **14**, 535–550 (1979).
- ²⁷R. D. H. Chu, G. VanDyke, D. F. Lewis, K. P. J. O'Hara, B. R. Buckland, and F. Dinelle, "GAFCHROMIC[®] dosimetry media: A new high dose rate thin film routine dosimeter and dose mapping tool," *Radiat. Phys. Chem.* **35**, 767–773 (1990).
- ²⁸M. J. Butson, K. N. Yu, T. Cheung, and P. E. Metcalfe, "Radiochromic film for Medical Radiation Dosimetry," *Mater. Sci. Eng., R.* **41**, 61–120 (2003).
- ²⁹M. J. Butson, J. N. Mathur, and P. E. Metcalfe, "Radiochromic film as a radiotherapy surface-dose detector," *Phys. Med. Biol.* **41**, 1073–1078 (1996).
- ³⁰M. J. Butson, P. K. N. Yu, and P. E. Metcalfe, "Measurement of off-axis dose and peripheral skin dose using radiochromic film," *Phys. Med. Biol.* **43**, 2647–2650 (1996).
- ³¹M. J. Butson, P. K. N. Yu, and P. E. Metcalfe, "Extrapolated surface dose measurements with radio-chromic film," *Med. Phys.* **26**, 485–488 (1999).
- ³²T. Cheung, M. J. Butson, P. K. N. Yu, "Multilayer Gafchromic film detectors for breast skin dose determination in vivo," *Phys. Med. Biol.* **47**, N31–N37 (2002).
- ³³S. Devic, J. Seuntjens, G. Hegyi, E. B. Podgorsak, C. G. Soares, A. S. Kirov, I. Ali, J. F. Williamson, and A. Elizondo, "Dosimetric properties of improved GafChromic films for seven different digitizers," *Med. Phys.* **31**, 2392–2401 (2004).
- ³⁴S. Devic, J. Seuntjens, E. Sham, E. B. Podgorsak, A. S. Kirov, R. C. Schmidlein, and C. G. Soares, "Precise radiochromic film dosimetry using a flat-bed document scanner," *Med. Phys.* **32**, 2245–2253 (2005).
- ³⁵C. Zankowski and E. B. Podgorsak, "Calibration of photon and electron beams with an extrapolation chamber," *Med. Phys.* **24**, 497–503 (1997).
- ³⁶W. Abdel-Rahman, J. P. Seuntjens, F. Verhaegen, F. Deblois, and E. B. Podgorsak, "Validation of Monte Carlo calculated surface doses for megavoltage photon beams," *Med. Phys.* **32**, 286–298 (1995).
- ³⁷I. Kawrakow and D. W. O. Rogers, "The EGSnrc code system: Monte Carlo simulation of electron and photon transport," Technical Report PIRS 701, National Research Council of Canada, Ottawa, Canada, 2000 (see <http://www.irs.inms.nrc.ca/inms/irs/EGSnrc/EGSnrc.html>).
- ³⁸W. O. Rogers, I. Kawrakow, J. P. Seuntjens, and B. R. B. Walters, "NRC user codes for EGSnrc," Technical Report PIRS702, National Research Council of Canada, Ottawa, Canada, 2000.
- ³⁹T. Kron and P. Ostwald, "Skin exit dose in megavoltage x-ray beams determined by means of a plane parallel ionization chamber (Attix chamber)," *Med. Phys.* **22**, 577–578 (1995).